Journal of Organometallic Chemistry, 372 (1989) 273–285
Elsevier Sequoia S.A., Lausanne – Printed in The Netherlands
JOM 09989

Competitive addition and substitution reactions in the interaction of $CpWOs_3(CO)_9(\mu\text{-}O)(\mu_3\text{-}CCH_2Tol)$ with phosphorus donors. The crystal structure of $CpWOs_3(CO)_8(PPh_2Me)(\mu\text{-}O)(\mu_3\text{-}CCH_2Tol)$

Yun Chi, John R. Shapley *

Department of Chemistry, University of Illinois, Urbana, Illinois 61801 (U.S.A.)

Melvyn Rowen Churchill * **and James C. Fettinger**

Department of Chemistry, University at Buffalo, S.U.N.Y., Buffalo, New York, 14214 (U.S.A.)

(Received September 8th, 1988)

Abstract

Treatment of a $CpWOs_3(CO)_9(\mu\text{-}O)(\mu_3\text{-}CCH_2Tol)$ (**1**) with excess trimethylphosphite in boiling toluene afforded both an addition product, $CpWOs_3(CO)_9(P(OMe)_3)(\mu\text{-}O)(\mu_3\text{-}CCH_2Tol)$ (**3**), and a substitution product, $CpWOs_3(CO)_8(P(OMe)_3)(\mu\text{-}O)(\mu_3\text{-}CCH_2Tol)$ (**4**), isolated as crystalline solids in 32% and 21% yields, respectively. From an analogous reaction of **1** with diphenylmethylphosphine only the substitution product $CpWOs_3(CO)_8(PPh_2Me)(\mu\text{-}O)(\mu_3\text{-}CCH_2Tol)$ (**5**) was isolated. Complexes **3–5** have been characterized by IR, ^1H and ^{13}C NMR, and field desorption mass spectroscopies. In addition the molecular structure of **5** has been determined by X-ray crystallography.

Introduction

We have previously reported the synthesis [1] and crystal structure [1,2] of the oxo-alkylidyne complex $CpWOs_3(CO)_9(\mu\text{-}O)(\mu_3\text{-}CCH_2Tol)$ (**1**). In examining the chemistry of **1** (see eq. 1), we have found that it adds one equivalent of carbon monoxide to form $CpWOs_3(CO)_{10}(\mu\text{-}O)(\mu_3\text{-}CCH_2Tol)$ (**2**) [3]. However, results with phosphorus donors show that **1** can undergo substitution as well as addition. In this paper we report the synthesis and characterization of the products from reaction of **1** with both trimethylphosphite (**3** and **4**) and diphenylmethylphosphine (**5**).

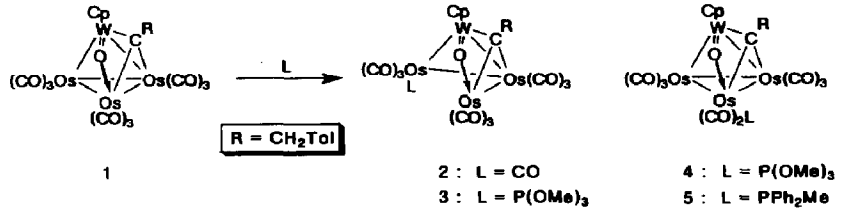

1

2 : L = CO
3 : L = P(OMe)3

4 : L = P(OMe)3
5 : L = PPh2Me

(1)

0022-328X/89/$03.50

Results and discussion

Two phosphite products were formed very quickly (less than three minutes) by treating **1** either with 1.5 equivalents or with 14 equivalents of $P(OMe)_3$ in refluxing toluene. Field desorption mass spectrometry indicated that one was an addition product, $CpWOs_3(CO)_8(P(OMe)_3)(\mu_3\text{-}CCH_2Tol)$ (**3**) and the other was the substitution product, $CpWOs_3(CO)_9(P(OMe)_3)(\mu\text{-}O)(\mu_3\text{-}CCH_2Tol)$ (**4**). Treatment of **1** with excess PPh_2Me in refluxing toluene provided a substitution product $CpWOs_3(CO)_8(PPh_2Me)(\mu\text{-}O)(\mu_3\text{-}CCH_2Tol)$ (**5**), for which the formulation was obtained by spectroscopic and analytical methods. An unstable product observed on the preparative TLC plate might be the addition product $CpWOs_3(CO)_9(PPh_2Me)(\mu\text{-}O)(\mu_3\text{-}CCH_2Tol)$, but this was not established.

Description of the crystal and molecular structure of $CpWOs_3(CO)_8(PPh_2Me)(\mu\text{-}O)(\mu_3\text{-}CCH_2Tol)$. Complex **5** crystallizes in the centrosymmetric triclinic space group $P\bar{1}$. Each molecule is chiral, but the crystal contains an ordered racemic array of the two enantiomeric forms. The overall molecular geometry and atomic labelling scheme are shown in Fig. 1, while Fig. 2 provides a stereoscopic view of the molecule. Interatomic distances and angles are collected in Tables 1 and 2.

The present molecule is derived from the parent compound **1** [1,2] by substitution of a PPh_2Me for a CO ligand on Os(1). The PPh_2Me ligand takes up a position *cis* to O(1) and *trans* to Os(3); it is situated such that it is displaced out of the W–Os(1)–Os(2) plane in the direction of the μ_3-alkylidyne ligand. In the following discussion bond lengths for the PPh_2Me-substituted species **5** are given first, followed by those of the parent compound **1** (in brackets).

The WOs_3 fragment forms a tetrahedral array as expected for a 60-electron tetranuclear cluster. Both Os–Os and W–Os bonds show wide variations, with

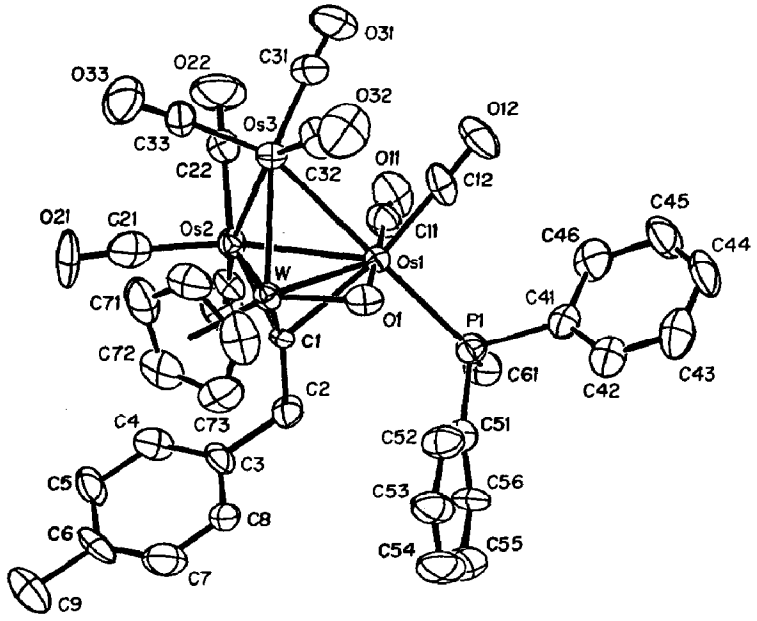

Fig. 1. Atomic vibration ellipsoids and the atomic labelling scheme for $CpWOs_3(CO)_8(PPh_2Me)(\mu\text{-}O)(\mu_3\text{-}CCH_2Tol)$ (**5**) (ORTEP diagram).

distances (in Å) being as follows: Os(1)–Os(2) 2.8276(7) [2.836(1)], Os(1)–Os(3) 2.9102(6) [2.875(1)], Os(2)–Os(3) 2.7532(7) [2.772(1)], W–Os(1) 2.6411(6) [2.663(1)], W–Os(2) 2.8348(6) [2.814(1)] and W–Os(3) 2.6570(6) [2.655(1)]. The μ-oxo ligand is involved in a W=O:→Os(1) bridge, in which W=O(1) is 1.810(8) Å [1.812(7) Å], Os(1)–O(1) 2.156(7) Å [2.169(8) Å] and angle W=O(1)–Os(1) is 83.04(29)° [83.46(31)°]. The μ_3-alkylidyne ligand spans the W–Os(1)–Os(2) face of the tetra-

Table 1

Interatomic distances (Å) and esd's for $CpWOs_3(CO)_8(PPh_2Me)(\mu\text{-}O)(\mu_3\text{-}CCH_2Tol)$

(A) Metal–metal distances:			
Os(1)–Os(2)	2.8276(7)	W–Os(1)	2.6411(6)
Os(1)–Os(3)	2.9102(6)	W–Os(2)	2.8348(6)
Os(2)–Os(3)	2.7532(7)	W–Os(3)	2.6570(6)
(B) Metal-alkylidyne, metal–oxygen and metal–phosphorus distances:			
W–C(1)	2.026(11)	W–O(1)	1.810(8)
Os(1)–C(1)	2.297(11)	Os(1)–O(1)	2.156(7)
Os(2)–C(1)	2.105(10)	Os(1)–P(1)	2.411(3)
(C) W–C and C–C distances for CpW moiety:			
W–C(71)	2.447(16)	C(71)–C(72)	1.388(21)
W–C(72)	2.409(15)	C(72)–C(73)	1.383(22)
W–C(73)	2.343(14)	C(73)–C(74)	1.439(24)
W–C(74)	2.323(14)	C(74)–C(75)	1.388(21)
W–C(75)	2.380(13)	C(75)–C(71)	1.376(23)
(D) Metal–carbonyl distances:			
Os(1)–C(11)	1.896(13)	Os(2)–C(23)	1.925(13)
Os(1)–C(12)	1.923(14)	Os(3)–C(31)	1.953(14)
Os(20–C(21)	1.879(15)	Os(3)–C(32)	1.889(15)
Os(2)–C(22)	1.941(13)	Os(3)–C(33)	1.853(13)
(E) Carbon–oxygen distances:			
C(11)–O(11)	1.137(16)	C(23)–O(23)	1.120(17)
C(12)–O(12)	1.160(17)	C(31)–O(31)	1.130(18)
C(21)–O(21)	1.154(19)	C(32)–O(32)	1.131(19)
C(22)–O(22)	1.133(17)	C(330–O(33)	1.157(17)
(F) Distances within the μ_3-CCH_2Tol ligand:			
C(1)–C(2)	1.530(16)	C(6)–C(7)	1.374(20)
C(2)–C(3)	1.553(17)	C(7)–C(8)	1.383(21)
C(3)–C(4)	1.381(18)	C(8)–C(3)	1.364(17)
C(4)–C(50	1.408(19)	C(6)–C(9)	1.539(21)
C(5)–C(6)	1.396(19)		
(G) Phosphorus–carbon distances:			
P(1)–C(41)	1.842(13)	P(1)–C(61)	1.850(13)
P(1)–C(51)	1.814(12)		
(H) Carbon–carbon distances within the PPh_2Me ligand:			
C(41)–C(42)	1.396(19)	C(51)–C(52)	1.369(18)
C(42)–C(43)	1.365(24)	C(52)–C(53)	1.386(18)
C(43)–C(44)	1.382(25)	C(53)–C(54)	1.340(21)
C(44)–C(45)	1.350(24)	C(54)–C(55)	1.372(25)
C(45)–C(46)	1.399(22)	C(55)–C(56)	1.373(19)
C(46)–C(41)	1.400(18)	C(56)–C(51)	1.411(18)

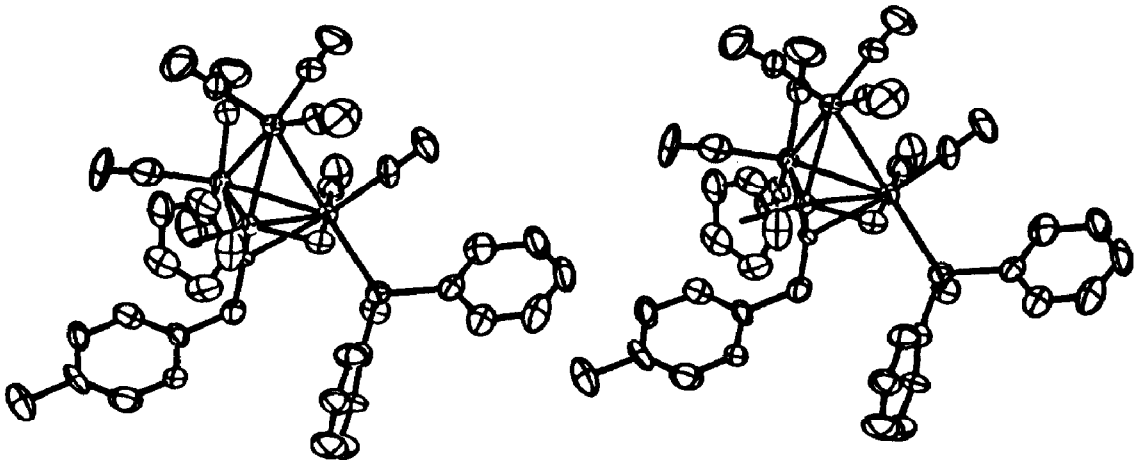

Fig. 2. A stereoscopic view of the $CpWOs_3(CO)_8(PPh_2Me)(\mu_3\text{-}CCH_2Tol)$ molecule.

hedral WOs_3 cluster with W–C(1) 2.026(11) Å [2.030(12) Å], Os(1)–C(1) 2.297(11) Å [2.291(12) Å], and Os(2)–C(1) 2.105(10) Å [2.100(10) Å].

The Os(1)–P(1) distance is 2.411(3) Å, but the presence of the phosphine ligand causes little perturbation in the remainder of the molecular architecture. Other distances are internally consistent and within the expected ranges, viz., Os–CO 1.853(13)–1.953(14) Å, C–O 1.120(17)–1.160(17) Å, W–C(Cp) 2.323(14)–2.447(16) Å (cf. ref [4]), C–C(Cp) 1.376(23)–1.439(24) Å, P–C 1.814(12)–1.850(13) Å, C–C(single bond) 1.530(16)–1.553(17) Å and C–C(aromatic) 1.340(21)–1.411(18) Å.

Spectroscopic characterization of the substitution products. The ^1H NMR spectra of **4** and **5** show resonances assignable to the diastereotopic methylene hydrogens of the alkylidyne ligand at δ 5.15 and 4.24 for **4** and at δ 4.71 and 3.35 for **5** in addition to the respective signals of the phosphorus ligand, Cp ligand, and the tolyl group. The alkylidyne α-carbon resonances in the ^{13}C NMR spectra are shifted upfield 6.6 ppm for **4** and 9.4 ppm for **5** from that observed at **1** at δ 220.8 [1]. This is consistent with the phosphorus ligand being bound to the oxo-osmium center, since the alkylidyne carbon resonance should not shift much if the new ligand were located at the remote, non-bridging osmium atom. No direct coupling between the phosphorus atom and the alkylidyne α-carbon is observed, however. The variable temperature ^{13}C NMR spectra of **4** and **5** (see Fig. 3) show evidence for localized exchange at each of the two $Os(CO)_3$ units but one unit is significantly more fluxional than the other. Similar behavior is observed also for **1** [3], and comparison of the resonances for all three compounds in Table 3 allows assignment of the set of carbonyls with the most upfield average shift to those attached to the oxo-osmium center.

Spectroscopic characterization of the phoshpite addition product. The characterization of **3** is more complicated and was hampered by the presence of a second form in solution. The relative ratio of these isomers (about 3/1) could not be altered by carrying out the recrystallization in different solvents. The mass spectrum establishes the overall composition, and the ^1H NMR spectrum of the major species shows all of the appropriate signals: Cp ligand at δ 5.82, inequivalent methylene protons at δ 6.27 and 5.30, phosphite methyls at δ 3.78, and tolyl methyl at δ 2.37.

Table 2

Interatomic angles (deg.) and esd's for $CpWOs_3(CO)_8(PPh_2Me)(\mu\text{-}O)(\mu_3\text{-}CCH_2Tol)$

(A) Intermetallic angles:			
Os(1)–W–Os(2)	62.06(2)	W–Os(2)–Os(1)	55.60(2)
Os(1)–W–Os(3)	66.64(2)	W–Os(2)–Os(3)	56.76(2)
Os(2)–W–Os(3)	60.07(2)	Os(1)–Os(2)–Os(3)	62.84(2)
W–Os(1)–Os(2)	62.33(2)	W–Os(3)–Os(1)	56.42(2)
W–Os(1)–Os(3)	56.94(2)	W–Os(3)–Os(2)	63.17(2)
Os(2)–Os(1)–Os(3)	57.33(2)	Os(1)–Os(3)–Os(2)	59.83(2)
Metal–metal–L angles: (L = P(1), O(1) or C(1))			
W–Os(1)–P(1)	116.89(8)	Os(1)–W–C(1)	57.17(30)
Os(2)–Os(1)–P(1)	131.33(8)	Os(2)–W–C(1)	48.75(30)
Os(3)–Os(1)–P(1)	167.89(8)	Os(3)–W–C(1)	101.91(30)
Os(1)–W–O(1)	54.11(24)	W–Os(1)–C(1)	47.81(26)
Os(2)–W–O(1)	116.14(24)	Os(2)–Os(1)–C(1)	47.12(26)
Os(3)–W–O(1)	91.79(24)	Os(3)–Os(1)–C(1)	88.45(26)
W–Os(1)–O(1)	42.85(20)	W–Os(2)–C(1)	45.51(29)
Os(2)–Os(1)–O(1)	105.17(20)	Os(1)–Os(2)–C(1)	53.09(29)
Os(3)–Os(1)–O(1)	78.59(20)	Os(3)–Os(2)–C(1)	96.80(29)
(C) Metal–metal–CO angles:			
W–Os(1)–C(11)	135.11(40)	W–Os(2)–C(23)	133.63(38)
Os(2)–Os(1)–C(11)	72.78(40)	Os(1)–Os(2)–C(23)	107.51(38)
Os(3)–Os(1)–C(11)	98.89(40)	Os(3)–Os(2)–C(23)	160.73(38)
W–Os(1)–C(12)	117.69(39)	W–Os(3)–C(31)	153.34(43)
Os(2)–Os(1)–C(12)	127.72(39)	Os(1)–Os(3)–C(31)	97.07(43)
Os(3)–Os(1)–C(12)	78.89(39)	Os(2)–Os(3)–C(31)	102.95(43)
W–Os(2)–C(21)	93.76(43)	W–Os(3)–C(32)	91.57(42)
Os(1)–Os(2)–C(21)	149.35(43)	Os(1)–Os(3)–C(32)	98.82(42)
Os(3)–Os(2)–C(21)	101.26(43)	Os(2)–Os(3)–C(32)	152.86(42)
W–Os(2)–C(22)	134.43(41)	W–Os(3)–C(33)	105.76(41)
Os(1)–Os(2)–C(22)	107.28(41)	Os(1)–Os(3)–C(33)	157.04(41)
Os(3)–Os(2)–C(22)	77.71(41)	Os(2)–Os(3)–C(33)	100.38(41)
(D) Metal–P(1)–carbon and carbon–P(1)–carbon angles:			
Os(1)–P(1)–C(41)	114.04(40)	C(41)–P(1)–C(51)	103.84(57)
Os(1)–P(1)–C(51)	118.53(42)	C(41)–P(1)–C(61)	101.38(57)
Os(1)–P(1)–C(61)	112.98(42)	C(51)–P(1)–C(61)	104.15(58)
(E) L–metal–L angles (L = P(1), O(1), or C(1))			
O(1)–W–C(1)	94.79(38)		
P(1)–Os(1)–O(1)	90.16(21)		
P(1)–Os(1)–C(1)	93.80(27)		
O(1)–Os(1)–C(1)	78.74(33)		
(F) L–Metal–CO angles: (L = P(1), C(1) or O(1))			
P(1)–Os(1)–C(11)	92.40(40)	C(1)–Os(1)–C(12)	165.17(47)
P(1)–Os(1)–C(12)	97.04(40)	C(1)–Os(2)–C(21)	107.96(52)
O(1)–Os(1)–C(11)	177.41(44)	C(1)–Os(2)–C(22)	158.74(50)
O(1)–Os(1)–C(12)	91.10(44)	C(1)–Os(2)–C(23)	88.74(47)
O(1)–Os(1)–C(11)	100.65(48)		
(G) CO–metal–CO angles:			
C(11)–Os(1)–C(12)	89.01(56)	C(31)–Os(3)–C(32)	95.80(60)
C(21)–Os(2)–C(22)	93.29(60)	C(31)–Os(3)–C(33)	98.94(59)
C(21)–Os(2)–C(23)	94.48(57)	C(32)–Os(3)–C(33)	95.82(59)
C(22)–Os(2)–C(23)	90.46(56)		

Table 2 (continued)

(H) Angles involving C(1) or O(1):			
W–C(1)–Os(1)	75.02(34)	Os(2)–C(1)–C(2)	129.17(77)
W–C(1)–Os(2)	86.63(40)	W–O(1)–Os(1)	83.04(29)
W–C(1)–C(2)	138.47(80)		
Os(1)–C(1)–Os(2)	79.79(35)		
Os(1)–C(1)–C(2)	125.42(75)		
(I) Metal–carbon–oxygen angles:			
Os(1)–C(11)–O(11)	175.3(12)	Os(2)–C(23)–O(23)	174.6(12)
Os(1)–C(12)–O(12)	178.8(12)	Os(3)–C(31)–O(31)	176.7(13)
Os(2)–C(21)–O(21)	174.8(13)	Os(3)–C(32)–O(32)	175.6(13)
Os(2)–C(22)–O(22)	175.8(13)	Os(3)–C(33)–O(33)	175.4(12)
(J) Carbon–carbon–carbon angles within the μ_3-CCH_2Tol Ligand:			
C(1)–C(2)–C(3)	113.1(10)	C(5)–C(6)–C(7)	118.0(13)
C(2)–C(3)–C(4)	121.4(11)	C(5)–C(6)–C(9)	119.1(12)
C(2)–C(3)–C(8)	120.4(11)	C(7)–C(6)–C(9)	122.8(13)
C(4)–C(3)–C(8)	118.1(12)	C(6)–C(7)–C(8)	121.1(13)
C(3)–C(4)–C(5)	120.7(12)	C(3)–C(8)–C(7)	121.8(12)
C(4)–C(5)–C(6)	120.0(12)		
(K) Phosphorus–carbon–carbon angles:			
P(1)–C(41)–C(42)	124.0(10)	P(1)–C(51)–C(52)	120.9(10)
P(1)–C(41)–C(46)	118.2(10)	P(1)–C(51)–C(56)	122.2(10)
(L) Carbon–carbon–carbon angles within phenyl rings:			
C(42)–C(41)–C(46)	117.8(12)	C(52)–C(51)–C(56)	116.8(12)
C(43)–C(42)–C(41)	120.7(14)	C(53)–C(52)–C(51)	123.1(13)
C(44)–C(43)–C(42)	120.8(16)	C(54)–C(53)–C(52)	118.4(14)
C(45)–C(44)–C(43)	120.1(16)	C(55)–C(54)–C(53)	121.3(15)
C(46)–C(45)–C(44)	120.3(15)	C(56)–C(55)–C(54)	120.4(15)
C(41)–C(46)–C(45)	120.3(13)	C(51)–C(56)–C(55)	119.8(13)
(M) Carbon–carbon–carbon angles within Cp ring:			
C(72)–C(71)–C(75)	107.5(13)	C(75)–C(74)–C(73)	106.9(13)
C(73)–C(72)–C(71)	109.8(13)	C(71)–C(75)–C(74)	109.6(13)
C(74)–C(73)–C(72)	106.3(13)		

Unfortunately, not all of the signals of the minor species could be resolved. The ^{13}C NMR spectrum of **3** shows assignable signals for the major species. As a whole the spectrum closely resembles that of **2** [3]. Definitive details are the alkylidyne signal (δ 219.7, J(WC) 109 Hz vs. δ 220.7, J(WC) 105 Hz), the presence of two strongly coupled carbonyls characteristic of *trans* positions in an $Os(CO)_2L_2$ group, and the fluxionality of three carbonyls (the signals at 187.7, 183.0, and 179.5 observed for **3** at $-45\,^{\circ}C$ broaden and disappear by room temperature). The signal for **3** located at 185.3 shows significant phosphorus coupling; the corresponding carbonyl ligand together with the phosphite ligand are assigned positions mutually *cis* to the *trans* carbonyls on the $Os(CO)_3P(OMe)_3$ group. Although definitive signals for the minor species could not be resolved, we expect it to result from a different location of the phosphite in this $Os(CO)_3L$ moiety.

Formation and interconversion of 3 and 4. A comparable ratio of **3** to **4** resulted regardless of the $P(OMe)_3$/**1** ratio (1.5 or 14 equiv.). Although the kinetics were not studied, this suggests that the rate laws controlling the formation of **3** and **4** have the

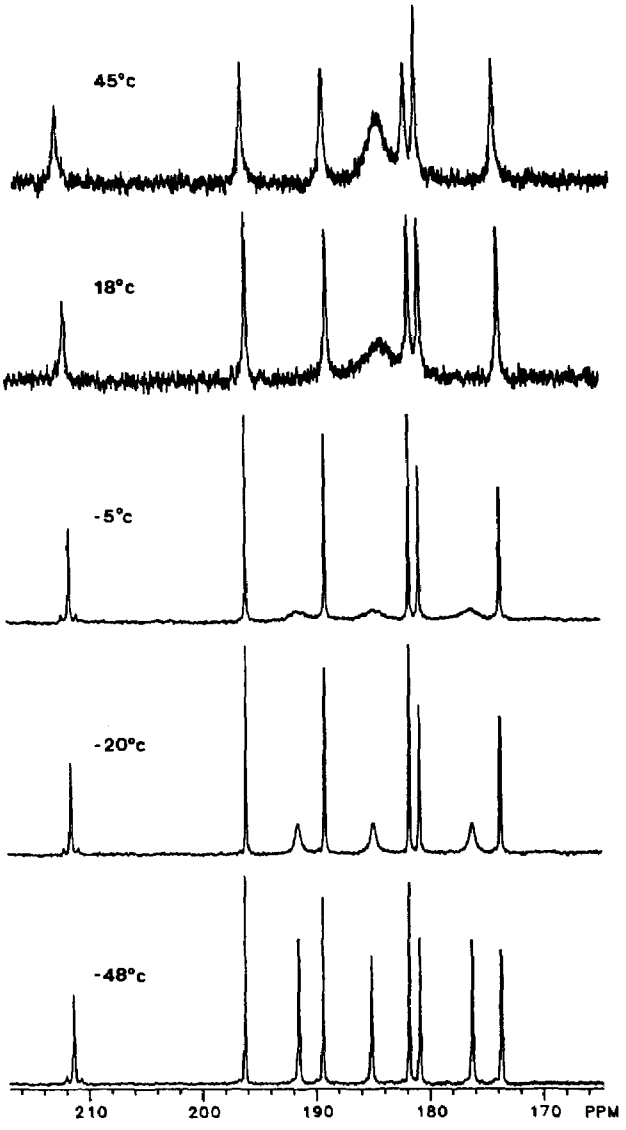

Fig. 3. Variable-temperature $^{13}C\{^1H\}$ NMR spectra (90MHz, $CDCl_3$) of $CpWOs_3(^*CO)_8(PPh_2Me)(\mu\text{-}O)(\mu_3\text{-}^*CCH_2Tol)$ (**5**). The carbonyl ligands are grouped into sets A, B, and C (see Table 3): group B is broad at $-20\,^\circ C$ and coalesced at $18\,^\circ C$, group A is losing intensity (broadening faster) relative to group C at $45\,^\circ C$.

Table 3

Carbonyl ^{13}C NMR resonances for compounds $CpWOs_3(CO)_8(L)(\mu\text{-}O)\mu_3\text{-}CCH_2Tol)$

Compound	L	Carbonyl resonances [a]		
		Set A	Set B	Set C [b]
1	CO	195.2, 187.7, 179.9	188.7, 182.5, 178.6	179.6, 175.0, 166.2
4	$P(OMe)_3$	196.2, 189.2, 181.6	190.8, 184.7, 176.3	181.4, 170.9 [c]
5	PPh_2Me	196.2, 189.3, 181.7	191.5, 185.1, 176.2	180.8, 173.6

[a] Grouped on the basis of barriers to local exchange: set B < set A < set C. [b] Assigned to the carbonyls attached to the oxo-osmium center (see text). [c] Note that this signal is a doublet due to P–C coupling.

same ligand dependence. At this point we choose not to speculate about a detailed mechanism, but the general transformation from a tetrahedral to a butterfly framework upon ligand addition is well known [5].

Pyrolysis of **3** in refluxing toluene produced **4** in moderate yield, although the rate at which this occurred was much slower than the rate at which the mixture of **3** and **4** was formed from **1**. The reverse transformation of **4** into **3** under 1 atm of carbon monoxide was also observed. Given the structural assignments of these two compounds, the transformation either involves phosphite migration or some extensive cluster rearrangement. Dissociative phosphite migration is contraindicated, since the pyrolysis of **4** in the presence of $P(OEt)_3$ gave only the substitution product $CpWOs_3(CO)_7(P(OMe)_3)(P(OEt)_3)(\mu\text{-}O)(\mu_3\text{-}CCH_2Tol)$, as indicated by mass spectrometry. This leaves the non-dissociative pathway as the most likely alternative, probably involving the migration of both oxo and alkylidyne ligands. In the clusters $(\mu\text{-}H)(M_3(\mu\text{-}CNMe_2)(CO)_9L$ ($M = Ru$, Os; $L = PR_3$, AsR_3, SbR_3) [6] migration of both the hydride and the μ-$CNMe_2$ ligand has been invoked to account for the equilibration of two structural isomers that differ in the location of the "marker" ligand L relative to the bridging carbyne ligand.

Experimental

General comments: All reactions were carried out under an atmosphere of nitrogen or argon in oven dried glassware. Solvents were dried before use. The progress of reactions was monitored by analytical thin-layer chromatography (silica gel TLC plates, Eastman). Preparative thin-layer plates were prepared from Silica Gel G (type 60, E. Merck). Complex **1** was prepared by the procedure described previously [1].

Field desorption mass spectra were recorded by the staff of the Mass Spectroscopy Laboratory of the School of Chemical Sciences at the University of Illinois using a Varian MAT-731 mass spectrometer. All m/z values are referenced to ^{184}W and ^{192}Os. Infrared spectra were obtained on a Perkin–Elmer 281B spectrophotometer. Both ^1H NMR (360 MHz) and ^{13}C NMR (90.4 MHz) spectra were recorded on a Nicolet NT-360 spectrometer. Microanalysis data were provided by the Microanalytical Laboratory of the School of Chemical Sciences at the University of Illinois.

Reaction of 1 with trimethylphosphite. A toluene solution (15 ml) of **1** (57 mg, 0.047 mmol) and 14 equiv. of $P(OMe)_3$ (80 mg, 0.64 mmol) was heated at reflux for three minutes. The solvent and excess phosphite were removed under vacuum. Preparative TLC (pentane/dichloromethane, 1/2) of the residue provided $CpWOs_3(CO)_9(P(OMe)_3)(\mu\text{-}O)(\mu_3\text{-}CCH_2Tol)$ (**3**) (19.7 mg, 0.015 mmol, 32%) and $CpWOs_3(CO)_8(P(OMe)_3)(\mu\text{-}O)(\mu_3\text{-}CCH_2Tol)$ (**4**) (13.1 mg, 0.010 mmol, 21%), in addition to several uncharacterized minor products. The relative amounts of **3** and **4** were unchanged when only 1.5 equiv. $P(OMe)_3$ was utilized with the same reaction conditions. Both **3** and **4** were purified by recrystallization from dichloromethane/pentane at room temperature.

$CpWOs_3(CO)_9(P(OMe)_3)(\mu\text{-}O)(\mu_3\text{-}CCH_2Tol)$ (**3**): Anal. Found: C, 23.06; H, 1.74. $W_1O_3C_{35}H_{27}O_{10}P_1$ calcd.: C, 23.50; H, 1.74%. FD mass spectrum, m/z 1344 (M^+). IR (C_6H_{12}): ν(CO), 2090(s), 2033(vs), 2026(vs), 2010(vs), 1994(m), 1982(m), 1970(s), 1947(sh,vw), 1934(br,m) cm^{-1}. ^1H NMR ($CDCl_3$, 18°C): δ 7.38 to 7.16

(4H, m, $C_6H_4CH_3$)*, 6.27 (1H, d, ^2J(H–H) 15 Hz, μ_3-CCH_2Tol)*, 5.94 (s, C_5H_5, minor), 5.82 (s, C_5H_5, major), 5.30 (1H, d, ^2J(H–H) 15 Hz, μ_3-CCH_2Tol)*, 3.81 (d, ^2J(P–H) 11 Hz, POCH_3, minor), 3.78 (d, ^2J(P–H) 11 Hz, POCH_3, major), 2.37 (s, $C_6H_5CH_3$)* (* signal for minor species not resolved). ^{13}C NMR (CD_2Cl_2, −45°C, signals for major species only): δ 219.7 (^1J(C–W) 109 Hz, μ_3-CCH_2Tol); δ 118.0, 187.7, 185.3 (^2J(P–C) 11 Hz), 185.0*, 184.5*, 183.7, 183.0, 179.5, 175.9 (* these signals have superimposed AB pattern with ^2J(CC) ~ 30 Hz).

$CpWOs_3(CO)_8(P(OMe)_3)(\mu$-O)($\mu_3$-C$CH_2$Tol) (**4**): Anal. Found: C, 22.75; H, 1.75. $W_1Os_3C_{35}H_{27}O_9P_1$ calcd.: C, 23.08; H, 1.78%. FD mass spectrum, m/z 1306 (M^+). IR (C_6H_{12}): ν(CO), 2055(s), 2020(vs), 2009(sh,w), 2002(m), 1986(w), 1968(s), 1950(s), 1940(w) cm^{-1} ^{1}H NMR ($CDCl_3$, 18°C): δ 7.25 to 7.13 (4H, m, $C_6H_4CH_3$), 5.64 (5H, s, C_5H_5), 5.15 (1H, d, ^2J(H–H) 15 Hz, μ_3-CCH_2Tol), 4.24 (1H, d, ^2J(H–H) 15 Hz, μ_3-CCH_2Tol), 3.76 (9H, d, ^2J(P–H) 11.7 Hz, POCH_3), 2.33 (3H, s, $C_6H_4CH_3$). ^{13}C NMR ($CDCl_3$, −24°C): δ 214.1 (^1J(C–W) 122 Hz, μ_3-CCH_2Tol); δ 196.2, 190.8(br), 189.2, 184.7(br), 181.6, 181.4, 176.3(br), 170.9 (^2J(P–C) 10 Hz) (all Os*CO*).

Pyrolysis of 3. A toluene solution (10 ml) of **3** (7.7 mg, 0.0058 mmol) was heated to reflux under a slow stream of argon for 2 h. The solvent was evaporated in vacuo, and the residue was separated by preparative TLC (pentane/dichloromethane, 1/2). Compound **4** (4.8 mg, 0.0037 mmol, 64%) was isolated as a red-brown solid. The remaining components were starting material (~ 0.5 mg) and a compound tentatively identified as the substituted hydrido-vinylidene complex $CpWOs_3(CO)_8(P(OMe)_3)(\mu$-O)($\mu$-H)($\mu$-C=CHTol) (~ 0.2 mg) on the basis of its FD mass spectrum (m/z 1306, M^+) and IR spectrum [1] (ν(CO) 2061(s), 2034(vs), 2018(s), 1988(s), 1979(s), 1964(vw), 1952(w), 1949(m) cm^{-1}).

Carbonylation of 4. A toluene solution (8 ml) of **4** (5.2 mg, 0.0040 mmol) was heated to reflux under 1 atm of carbon monoxide for 6 h. The solvent was evaporated in vacuo, and the residue was separated by preparative TLC (pentane/dichloromethane, 1/2). Small amounts of **3** (~ 0.4 mg) and of $CpWOs_3(CO)_8(P(OMe)_3)(\mu$-O)($\mu$-H)($\mu$-C=CHTol) (0.2 mg) (see above) were isolated in addition to recovery of **4** (3.5 mg, 67%).

Reaction of 1 with diphenylmethylphosphine. A toluene solution (18 ml) of **1** (53.5 mg, 0.044 mmol) and PPh_2Me (40 mg, 0.2 mmol), was heated at reflux for 20 minutes. The solvent was evaporated and the residue was separated by preparative TLC (pentane/dichloromethane, 1/2), giving $CpWOs_3(CO)_8(PPh_2Me)(\mu$-O)($\mu_3$-C$CH_2$Tol) (**5**) (30.2 mg, 0.022 mmol, 50%) as a red crystalline solid after crystallization from hot chloroform/heptane. One unidentified component of the reaction mixture was found to decompose upon contact with silica gel during the TLC separation.

$CpWOs_3(CO)_8(PPh_2Me)(\mu$-O)($\mu_3$-C$CH_2$Tol) (**5**): Anal. Found: C, 29.88; H, 1.96. $W_1Os_3C_{35}H_{27}O_9P_1$ calcd.: C, 30.53; H, 1.96%. FAB mass spectrum, m/z 1382 (M^+). IR (C_6H_{12}): ν(CO), 2051(s) 2016(vs), 1999(m), 1967(s), 1947(m) cm^{-1}. ^{1}H NMR ($CDCl_3$, 18°C): δ 7.50 to 7.42 (10H, m, PC_6H_5), 7.06 to 6.86 (4H, m, $C_6H_4CH_3$), 5.58 (5H, s, C_5H_5), 4.71 (1H, ^2J(H–H) 15.2 Hz, μ_3-CCH_2Tol), 3.35 (1H, d, ^2J(H–H) 15.2 Hz, μ_3-CCH_2Tol), 2.28 (3H, s, $C_6H_4CH_3$), 2.24 (3H, d, ^2J(P–H) 9.2 Hz, PCH_3). ^{13}C NMR ($CDCl_3$, −48°C): δ 211.3 (^1J(C–W) 110 Hz, μ_3-CCH_2Tol); δ 196.2, 191.5, 189.3, 185.1, 181.7, 180.8, 176.2, 173.6 (all Os*CO*).

Collection of X-ray diffraction data for $CpWOs_3(CO)_8(PPh_2Me)(\mu$-O)($\mu_3$-C$CH_2$Tol)

Table 4

Experimental data for the X-ray diffraction study of $CpWOs_3(CO)_8(PPh_2Me)(\mu\text{-}O)(\mu_3\text{-}CCH_2Tol)$

(A) Unit cell data	
a 10.111(5) Å	crystal system: triclinic
b 11.732(4) Å	space group: $P\bar{1}$ (No. 2)
c 16.836(6) Å	$Z = 2$
α 78.508(25)°	formula: $C_{35}H_{27}O_9Os_3PW$
β 79.408(31)°	mol. wt. = 1377.1
γ 66.321(26)°	D(calc'd) = 2.57 g/cm^3
V 1780.3(11) Å^3	T 24°C (276 K)

(B) Collection of X-ray diffraction data

Diffractometer: Syntex $P2_1$

Radiation: Mo-K_α($\bar{\lambda}$ 0.710730 Å)

monochromator: highly orientated (pyrolytic) graphite; equatorial mode with 2θ(m) = 12.160°; assumed to be 50% perfect/50% ideally mosaic for polarization correction.

reflections meas'd: $+h, \pm k, \pm l$ for 2θ 4.5–45.0°, yielding 4673 unique data (none rejected).

scan type: coupled θ(crystal)–2θ(counter)

scan width: $[2\theta(K_{\alpha_1}) - 0.9]° \rightarrow [2\theta(K_{\alpha_2}) + 0.9]°$

scan speed: 4.0 deg/min (2θ)

backgrounds: stationary-crystal, stationary-counter at the two extremes of the 2θscan; each for one-quarter of the total scan time.

standard reflns: three mutually orthogonal reflections collected before each set of 97 data points. No decay observed.

absorption correction: μ(Mo-K_α) = 148.1 cm^{-1}; corrected empirically by interpolation (in 2θ and ϕ) between 3 close-to-axial (ψ-scan) reflections.

(5). A dark red crystal of approximate dimensions $0.13 \times 0.20 \times 0.33$ mm was sealed (in air) into a glass capillary. This was mounted in a eucentric goniometer and was accurately centered on a Syntex $P2_1$ automated four-circle diffractometer with the extended crystal direction approximately coincident with the ϕ-axis. All subsequent set-up operations (i.e., determination of cell parameters and orientation matrix) and collection of the X-ray diffraction data were carried out as described previously [7]. Details appear in Table 4. The final cell parameters are based upon a least-squares fit of the setting angles (2θ, ω, χ) of the unresolved Mo-$K_{\bar{\alpha}}$ components of 25 reflections well-dispersed in reciprocal space and with 2θ in the range 20–30°. The diffraction symmetry ($\bar{1}$, C_i) and the absence of any systematic extinctions indicated that the crystal belonged to the triclinic system, i.e.,space group $P1$ or $P\bar{1}$. The unit cell volume is consistent with $Z = 2$; this, combined with the intensity statistics, strongly suggest that the crystal belongs to the centrosymmetric space group $P\bar{1}$. This was assumed and was later confirmed by the successful solution of the structure in this higher-symmetry space group.

All data were corrected for the effects of absorption and for Lorentz and polarization factors. Symmetry-equivalent data were averaged ($R(I) = 3.0\%$ for 317 pairs of reflections) and all data were converted to unscaled $|F_o|$ values; any reflection with I(net) < 0 was assigned the value $|F_o| = 0$. Data were placed on an approximately absolute scale by means of a Wilson plot, which also provided the average overall isotropic thermal parameter, $\bar{B} = 2.49$ Å^2.

Solution and refinement of the structure of $CpWOs_3(CO)_8(PPh_2Me)(\mu\text{-}O)(\mu_3\text{-}CCH_2Tol)$ (5). All subsequent calculations were performed using our locally mod-

Table 5

Final positional parameters for $CpWOs_3(CO)_8(PPh_2Me)(\mu\text{-}O)(\mu_3\text{-}CCH_2Tol)$.

Atom	x	y	z	Atom	x	y	z
W	0.10002(5)	0.19044(4)	0.15106(3)	H(2A)	−0.1600	0.3662	0.2995
OS(1)	0.18248(4)	0.12872(4)	0.29892(3)	H(2B)	−0.2126	0.2594	0.3421
OS(2)	0.01741(4)	0.00615(4)	0.25982(3)	H(4)	−0.3570	0.1948	0.2571
OS(3)	0.29236(5)	−0.04347(4)	0.17792(3)	H(5)	−0.5389	0.2724	0.1689
P(1)	0.11543(31)	0.29737(27)	0.37852(19)	H(9A)	−0.7465	0.5106	0.1136
O(1)	0.21029(76)	0.25196(61)	0.18933(45)	H(9B)	−0.6382	0.4390	0.0454
C(1)	−0.0421(10)	0.20118(87)	0.25389(68)	H(9C)	−0.6571	0.5753	0.0504
C(2)	−0.1812(12)	0.2980(11)	0.29121(72)	H(7)	−0.4877	0.6038	0.1225
C(3)	−0.3066(11)	0.3497(11)	0.23648(72)	H(8)	−0.3039	0.5231	0.2061
C(4)	−0.3810(12)	0.2774(11)	0.22802(81)	H(42)	0.2493	0.4877	0.3569
C(5)	−0.4921(12)	0.3246(12)	0.17665(85)	H(43)	0.4438	0.4950	0.4059
C(6)	−0.5334(11)	0.4480(13)	0.13700(80)	H(44)	0.5892	0.3230	9.4883
C(7)	−0.4612(15)	0.5196(12)	0.14882(93)	H(45)	0.5364	0.1451	0.5248
C(8)	−0.3506(12)	0.4708(10)	0.19838(84)	H(46)	0.3391	0.1340	0.4768
C(9)	−0.6555(13)	0.4978(15)	0.03142(93)	H(52)	0.1333	0.4483	0.2251
C(11)	0.1589(12)	0.0148(11)	0.39233(80)	H(53)	0.0015	0.6484	0.1629
C(12)	0.3876(13)	0.0614(11)	0.30770(75)	H(54)	−0.2053	0.7734	0.2335
C(21)	−0.0776(13)	−0.0197(11)	0.1831(10)	H(55)	−0.2694	0.7116	0.3692
C(22)	0.1147(13)	−0.1724(12)	0.29453(87)	H(56)	−0.1449	0.5094	0.4309
C(23)	−0.1370(12)	0.0143(11)	0.34731(78)	H(61A)	−0.0828	0.2746	0.4671
C(31)	0.4128(14)	−0.1893(12)	0.24692(93)	H(61B)	−0.0117	0.3409	0.5070
C(32)	0.4462(14)	0.0047(13)	0.12272(79)	H(61G)	0.0588	0.1964	0.5074
C(33)	0.2841(12)	−0.1243(12)	0.09605(83)	H(71)	0.0065	0.0955	0.0220
O(11)	0.15365(95)	−0.05407(87)	0.44970(62)	H(72)	−0.1850	0.2797	0.0820
O(12)	0.51173(91)	0.01912(89)	0.31223(65)	H(73)	−0.0814	0.4411	0.0806
				H(74)	0.1848	0.3520	0.0164
O(21)	−0.1438(12)	−0.0267(10)	0.13647(59)	H(75)	0.2324	0.1395	−0.0171
O(22)	0.1640(11)	−0.27644(88)	0.31782(79)				
O(23)	−0.2303(10)	0.0142(10)	0.39491(63)				
O(31)	0.4789(11)	−0.27084(93)	0.29003(71)				
O(32)	0.5325(11)	0.0383(11)	0.08612(78)				
O(33)	0.2755(12)	−0.1669(10)	0.04176(66)				
C(41)	0.2708(12)	0.3110(11)	0.41259(72)				
C(42)	0.3063(14)	0.4174(12)	0.39153(85)				
C(43)	0.4222(17)	0.4213(15)	0.4201(10)				
C(44)	0.5083(13)	0.3194(17)	0.4694(10)				
C(45)	0.4776(13)	0.2148(15)	0.4906(10)				
C(46)	0.3594(15)	0.2084(13)	0.46228(78)				
C(51)	0.0123(12)	0.4562(11)	0.33394(78)				
C(52)	0.0497(13)	0.5011(11)	0.25526(81)				
C(53)	−0.0286914)	0.6199(11)	0.21744(92)				
C(54)	−0.1479(16)	0.6935(12)	0.2595(11)				
C(55)	−0.1885(15)	0.6555(13)	0.3394(11)				
C(56)	−0.1130(12)	0.5370(10)	0.37663(85)				
C(61)	0.0067(13)	0.2745(11)	0.47706(75)				
C(71)	0.0180(16)	0.1696(14)	0.02863(90)				
C(72)	−0.0881(14)	0.2723(13)	0.06189(74)				
C(73)	−0.0318(17)	0.3622(12)	0.06129(81)				
C(74)	0.1170(16)	0.3122(14)	0.02555(82)				
C(75)	0.1426(14)	0.1945(13)	0.00693(77)				

Table 6

Anisotropic thermal parameters (B_{ij}'s, in Å^2) for $CpWOs_3(CO)_8(PPh_2Me)(\mu\text{-}O)(\mu_3\text{-}CCH_2Tol)$.

Atom	B_{11}	B_{22}	B_{33}	B_{12}	B_{13}	B_{23}
W	2.288(20)	2.106(19)	1.998(22)	−0.771(15)	−0.351(15)	−0.138(15)
OS(1)	1.920(19)	2.088(19)	2.130(22)	−0.710(15)	−0.430(15)	−0.251(15)
OS(2)	2.240(20)	2.203(20)	2.516(23)	−0.981(15)	−0.467(16)	−0.138(16)
OS(3)	2.121(20)	2.418(20)	3.005(25)	−0.409(16)	−0.264(16)	−0.842(17)
P(1)	2.62(13)	2.74(13)	2.40(15)	−0.99(11)	−0.15(10)	−0.49(11)
O(1)	3.32(35)	1.85(30)	2.28(37)	−1.19(27)	−0.06(28)	0.81(26)
C(1)	1.23(40)	1.47(41)	3.13(56)	−0.06(33)	−0.75(37)	−0.50(38)
C(2)	2.48(50)	3.92(58)	2.65(58)	−1.18(44)	0.49(41)	−1.72(47)
C(3)	1.36(44)	3.92(60)	2.94(60)	−0.50(42)	−0.34(39)	−1.10(47)
C(4)	2.87(55)	3.05(55)	4.10(71)	−0.82(45)	−0.28(48)	−0.06(50)
C(5)	2.58(54)	4.51(66)	4.78(75)	−1.85(49)	−1.34(50)	−0.39(57)
C(6)	1.15(45)	5.31(72)	3.70(68)	−0.32(47)	−0.69(42)	−0.17(56)
C(7)	4.64(72)	3.42(62)	4.99(84)	−0.28(55)	−1.16(61)	−0.53(57)
C(8)	2.39(51)	2.53(54)	5.56(79)	−0.44(43)	−1.03(50)	−1.46(52)
C(9)	3.82(67)	7.34(91)	4.36(81)	−1.40(64)	−2.02(58)	0.25(69)
C(11)	3.15(56)	3.28(57)	2.63(63)	−0.86(46)	−0.75(45)	−0.09(50)
C(12)	3.26(61)	4.27(61)	2.97(63)	−2.51(50)	−1.29(46)	0.90(49)
C(21)	3.48(60)	2.81(56)	5.86(87)	−2.03(49)	0.35(57)	0.10(55)
C(22)	2.97(56)	3.23(63)	5.02(77)	−1.02(49)	−1.21(51)	−0.80(55)
C(23)	2.00(50)	3.25(54)	2.91(61)	−0.72(42)	−0.87(45)	0.01(45)
C(31)	3.46(60)	2.57(56)	5.50(83)	−0.48(49)	−1.11(56)	−0.86(56)
C(32)	3.16(59)	5.11(69)	2.60(62)	−1.75(53)	0.05(47)	−0.41(52)
C(33)	2.87(55)	3.89(60)	3.70(69)	−1.16(46)	−0.79(47)	−1.29(54)
O(11)	5.03(49)	5.06(48)	4.46(55)	−3.15(41)	−1.22(40)	1.06(43)
O(12)	2.26(41)	6.05(53)	6.97(66)	−1.02(37)	−1.62(39)	−0.71(46)
O(31)	8.13(63)	7.67(62)	3.60(50)	−5.40(54)	−2.66(46)	−0.42(44)
O(22)	6.26(59)	2.63(45)	10.35(90)	−1.08(43)	−2.08(56)	0.97(49)
O(23)	3.67(45)	7.30(60)	4.46(54)	−2.93(43)	−0.06(40)	0.09(45)
O(31)	5.64(55)	4.45(50)	6.62(68)	0.62(44)	−3.10(50)	−0.54(48)
O(32)	5.05(56)	8.76(73)	8.39(82)	−3.99(55)	2.38(53)	−3.31(62)
O(33)	7.57(64)	6.02(56)	4.57(59)	−2.34(49)	−1.14(47)	−1.93(48)
C(41)	2.81(52)	3.31(55)	2.79(60)	−1.57(44)	0.38(43)	−1.06(47)
C(42)	4.33(66)	4.69(68)	3.97(73)	−2.28(56)	−0.12(53)	−1.16(56)
C(43)	6.05(86)	6.69(90)	5.87(95)	−4.17(77)	−0.60(72)	−1.79(76)
C(44)	2.09(58)	9.1(11)	5.49(90)	−1.55(67)	−0.68(56)	−3.55(82)
C(45)	2.53(58)	6.22(82)	5.72(89)	−1.20(57)	−1.27(55)	−1.44(68)
C(46)	5.48(73)	4.86(70)	2.16(62)	−1.79(59)	−0.51(53)	−0.71(54)
C(51)	2.71(52)	2.93(53)	3.62(67)	−1.13(44)	−0.80(45)	−0.59(47)
C(52)	3.98(62)	3.36(61)	3.22(69)	−0.63(50)	0.13(50)	−0.78(52)
C(53)	3.36(61)	2.70(57)	5.97(86)	−1.16(50)	−0.60(56)	0.16(57)
C(54)	5.05(78)	2.18(57)	7.1(11)	−0.96(56)	−1.27(71)	0.77(62)
C(55)	4.22(71)	4.19(73)	6.2(10)	−0.44(58)	0.97(64)	−2.10(70)
C(56)	2.65(53)	2.06(51)	5.12(76)	0.35(43)	−1.02(49)	0.82(50)
C(61)	3.64(58)	3.56(58)	2.67(62)	−1.16(47)	−0.29(46)	−0.12(48)
C(71)	5.25(76)	5.32(77)	4.19(77)	−2.66(66)	−2.39(62)	0.56(63)
C(72)	4.86(70)	4.77(71)	1.36(56)	−1.04(60)	−0.89(49)	1.16(51)
C(73)	7.28(91)	2.79(58)	2.43(65)	−0.69(61)	−1.86(61)	0.76(49)
C(74)	6.47(85)	6.17(82)	2.67(65)	−5.12(72)	−1.02(59)	2.34(60)
C(75)	3.88(65)	4.56(70)	2.13(61)	−0.29(54)	−0.22(47)	−0.02(51)

ified version of the Syntex XTL set of interactive crystallographic programs [8]. The structure was solved by means of a Patterson map, which revealed the locations of four metal atoms; all were initially defined as osmium atoms. The positions of the remaining non-hydrogen atoms were determined from a difference-Fourier map. The identity of the tungsten atom was established from the Cp ligand attached to it. (With $Z(W) = 74$ and $Z(Os) = 76$, methods such as occupancy refinement are not very helpful in distinguishing relative atomic identities.) The hydrogen atoms of the methyl groups were located on subsequent difference-fourier maps. These and the other hydrogen atoms were input in idealized positions based upon d(C–H) 0.95 Å and the appropriate trigonal or tetrahedral geometry [9*]; the positions of these atoms were subsequently updated but were not refined. The structure was optimized by full-matrix leastsquares refinement of the residual $\Sigma w(|F_o| - |F_c|)^2$, where $1/w = \{[\sigma(|F_o|)]^2 + [0.015|F_o|]^2\}$. Positional and anisotropic thermal parameters of all non-hydrogen atoms were refined, leading to convergence with [10] R_F 4.1%, R_{wF} 3.8% and GOF 1.49 for all 4673 reflections (R_F 2.9%, R_{wF} 3.5% for those 3845 reflections with $|F_o| > 6\sigma(|F_o|)$). A final difference-Fourier map showed peaks of height 1.5–2.1 $e^-/Å^3$ within 1.2 Å of the metal atom positions, but no other extraneous features. Final positional and thermal parameters are collected in Tables 5 and 6.

Throughout the analysis, the values of F_c were calculated from analytical expressions for the scattering factors of neutral atoms; both the real ($\Delta f'$) and imaginary ($i\Delta f''$) components of anomalous dispersion were included for all non-hydrogen atoms [10].

Additional material

A Table of observed and calculated structure factor amplitudes is available upon request from one of us (M.R.C.).

Acknowledgements

This research was supported at the University of Illinois by National Science foundation grant CHE 84-07233.

References

1 J.R. Shapley, J.T. Park, M.R. Churchill, J.W. Ziller and L.R. Beanan, J. Am. Chem. Soc., 106 (1984) 1144.
2 M.R. Churchill, J.W. Ziller and L.R. Beanan, J. Organomet. Chem., 287 (1985) 235.
3 Y. Chi, J.R. Shapley and M.R. Churchill, Organometallics, submitted.
4 C. Bueno and M.R. Churchill, Inorg. Chem., 20 (1981) 2197.
5 E. Sappa, A. Tiripicchio, A.J. Carty and G.E. Toogood, Prog. Inorg. Chem., 34 (1986) 437.
6 M.A. Shaffer and J.B. Keister, Organometallics, 5 (1986) 561.
7 M.R. Churchill, R.A. Lashewycz and F.J. Rotella, Inorg. Chem., 16 (1977) 265.
8 Syntex XTL Operations Manual, Syntex Analytical Instruments, Cupertino, California 1976.
9 M.R. Churchill, Inorg. Chem., 12 (1973) 1213. $R_F = 100\Sigma||F_o| - |F_c||/\Sigma|F_o|$; $R_{wF} = 100[\Sigma w(|F_o| - |F_c|)^2/\Sigma w|F_o|^2]^{1/2}$; and $GOF = [\Sigma w(|F_o| - |F_c|)^2/(NO-NV)]^{1/2}$, where NO = number of observations and NV = number of variables.
10 "International Tables for X-Ray Crystallography", Kynoch Press, Birmingham, England, Volume 4, 1974, p. 99–101 and 149–150.

* Reference number with asterisk indicates a note in the list of references.